Physics Letters A 378 (2014) 755–759

Contents lists available at ScienceDirect

Physics Letters A

www.elsevier.com/locate/pla

Transmission of electric dipole radiation through an interface

Henk F. Arnoldus [a,*], Matthew J. Berg [a], Xin Li [b]

[a] Department of Physics and Astronomy, Mississippi State University, P.O. Drawer 5167, Mississippi State, MS 39762-5167, USA
[b] Department of Physics, P.O. Box 1002, Millersville University, Millersville, PA 17551, USA

ARTICLE INFO

Article history:
Received 19 December 2013
Accepted 10 January 2014
Available online 15 January 2014
Communicated by V.M. Agranovich

Keywords:
Reflection
Transmission
Poynting vector
Optical vortex
Angular spectrum
Fresnel coefficients
Dipole radiation

ABSTRACT

We consider the transmission of electric dipole radiation through an interface between two dielectrics, for the case of a vertical dipole. Energy flows along the field lines of the Poynting vector, and in the optical near field these field lines are curves (as opposed to optical rays). When the radiation passes through the interface into a thicker medium, the field lines bend to the normal (as rays do), but the transmission angle is not related to the angle of incidence. The redirection of the radiation at the interface is determined by the angle dependence of the transmission coefficient. This near-field redistribution is responsible for the far-field angular power pattern. When the transmission medium is thinner than the embedding medium of the dipole, some energy flows back and forth through the interface in an oscillating fashion. In each area where field lines dip below the interface, an optical vortex appears just above the interface. The centers of these vortices are concentric singular circles around the dipole axis.

1. Introduction

A light ray incident upon an interface reflects and refracts, with the angle of reflection equal to the angle of incidence, and the angle of refraction (transmission) given by Snell's law. When the angle of incidence is larger than the critical angle (for reflection at a thinner medium), there is no transmitted ray (total reflection). This ray description is valid for incoherent light on a macroscopic scale. In nano-photonics, where spatial resolution on the scale of a wavelength is of concern, this simple picture needs to be refined. Rather than viewing light as a bundle of optical rays, we need to consider the flow lines of electromagnetic energy, which are the field lines of the Poynting vector. For instance, when a light beam of finite cross section undergoes total reflection at a thinner medium, the center of the beam shifts parallel to the surface, which is known as the Goos–Hänchen shift [1]. In addition, an interference vortex in the energy flow lines appears in the thicker medium, and very close to the interface [2].

Both this shift and vortex are of sub-wavelength dimension, and are due to the finite cross section of the beam. Fig. 1 shows the field lines of the Poynting vector for a p-polarized plane wave incident under 30° from vacuum on an interface with a medium with index of refraction $n_2 = 2$. The scale is normalized with the wave number k_0 in vacuum, so $\bar{z} = k_0 z$, etc. Therefore, a distance of 2π corresponds to an optical wavelength. Snell's law gives $\theta_t = 14.5°$ for the transmission angle, and we see that indeed the field lines of energy flow emerge from the interface under angle θ_t. The field lines are straight, and indistinguishable from optical rays. The field in $\bar{z} < 0$ is a superposition of the incident and the reflected field. The angle of reflection for an infinite wave is equal to the angle of incidence, but due to the superposition the interpretation in terms of optical rays cannot be seen anymore. It appears that the energy flows to the interface under an angle larger than θ_i, and the field lines are wavy. Moreover, all energy flows towards the interface and transmits into the region $\bar{z} > 0$, giving the impression that there is no reflection at all.

We shall consider an oscillating electric dipole, embedded in a medium with relative permittivity ε_1, as shown in Fig. 2. The dipole is located on the z axis, a distance H below an interface (xy plane) with a medium with relative permittivity ε_2. We shall assume that ε_1 and ε_2 are positive. The emitted electric field by the dipole (source) is $\mathbf{E}_s$, and $\mathbf{E}_r$ and $\mathbf{E}_t$ indicate the reflected and transmitted fields, respectively. In the region $\bar{z} < 0$, the superposition of $\mathbf{E}_s$ and $\mathbf{E}_r$ gives interference. For a reflecting surface (mirror) this interference gives rise to the appearance of numerous singularities and vortices [3], and the mechanism of emission is fundamentally altered [4]. In the present paper we include transmission into the second medium, as a generalization of the mirror problem. The assumption that ε_1 and ε_2 are positive is non-essential, but is made here for simplicity of presentation.

* Corresponding author. Tel.: +1 662 325 2919; fax: +1 662 325 8898.
E-mail addresses: hfa1@msstate.edu (H.F. Arnoldus), matt.berg@msstate.edu (M.J. Berg), Xin.Li@millersville.edu (X. Li).

0375-9601/$ – see front matter
http://dx.doi.org/10.1016/j.physleta.2014.01.011

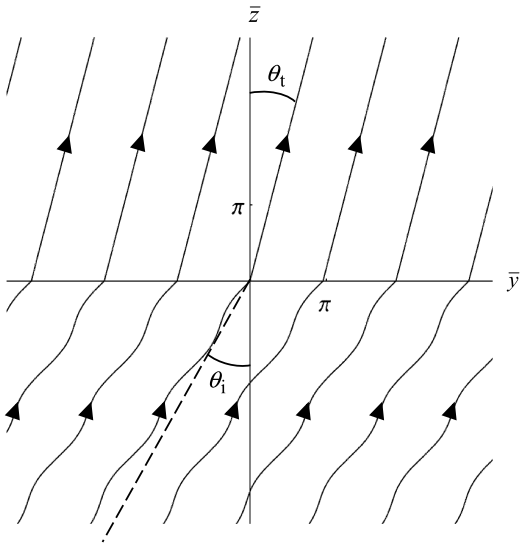

Fig. 1. The figure shows the field lines of the Poynting vector for a p-polarized plane wave incident upon an interface under angle $\theta_i = 30°$. The wave enters from vacuum, and the material in $\bar{z} > 0$ has index of refraction $n_2 = 2$. The energy in the transmitted wave flows along straight lines, and into the direction given by Snell's law. In the region $\bar{z} < 0$ the incident wave interferes with the reflected wave. The energy approaches the interface along a wavy path, and under an angle larger than the angle of incidence θ_i. The reflection coefficient is $R_p = 0.28$.

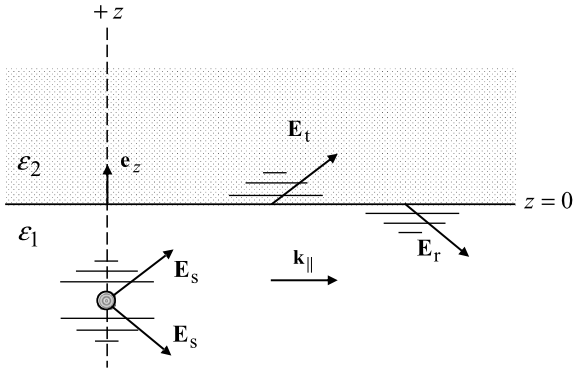

Fig. 2. An electric dipole is embedded in a medium with relative permittivity ε_1, and is located a distance H blow an interface with a medium with relative permittivity ε_2. The interface is the xy plane, and the positive z axis is taken as up. The part of the source field $\mathbf{E}_s$ that travels towards the interface gives rise to reflection and transmission. Each wave can be traveling or evanescent, which is schematically represented by an arrow and parallel lines, respectively.

2. Source field

When an electric dipole moment oscillates with angular frequency ω, the dipole moment can be written as $\mathbf{d}(t) = d_o \,\mathrm{Re}[\hat{\mathbf{u}} \exp(-i\omega t)]$, with $d_o > 0$ and $\hat{\mathbf{u}}^* \cdot \hat{\mathbf{u}} = 1$. The emitted electric field is of the form

$$\mathbf{E}_s(\mathbf{r}, t) = \mathrm{Re}\big[\mathbf{E}_s(\mathbf{r}) e^{-i\omega t}\big], \tag{1}$$

with $\mathbf{E}_s(\mathbf{r})$ the complex amplitude. Other fields have a similar time dependence. For the source field we have

$$\mathbf{E}_s(\mathbf{r}) = \varsigma \left\{ \hat{\mathbf{u}} - (\hat{\mathbf{q}}_1 \cdot \hat{\mathbf{u}})\hat{\mathbf{q}}_1 + \big[\hat{\mathbf{u}} - 3(\hat{\mathbf{q}}_1 \cdot \hat{\mathbf{u}})\hat{\mathbf{q}}_1\big] \frac{i}{n_1 q_1} \left(1 + \frac{i}{n_1 q_1}\right) \right\} \times \frac{e^{i n_1 q_1}}{q_1}, \tag{2}$$

where $n_1 = \sqrt{\varepsilon_1}$ is the index of refraction of the embedding medium and $k_o = \omega/c$. The overall constant is

$$\varsigma = \frac{k_o^3 d_o}{4\pi \varepsilon_o}. \tag{3}$$

The position vector of the field point $\mathbf{r}$ with respect to the location of the dipole is $\mathbf{r}_1 = \mathbf{r} + H\mathbf{e}_z$. We use the dimensionless position vector $\mathbf{q}_1 = k_o \mathbf{r}_1$, with magnitude $q_1 = |\mathbf{q}_1|$, and the corresponding unit vector is $\hat{\mathbf{q}}_1 = \mathbf{q}_1/q_1$. The complex amplitude of the emitted magnetic field is

$$\mathbf{B}_s(\mathbf{r}) = \frac{\varsigma}{c} n_1 (\hat{\mathbf{q}}_1 \times \hat{\mathbf{u}}) \left(1 + \frac{i}{n_1 q_1}\right) \frac{e^{i n_1 q_1}}{q_1}. \tag{4}$$

In order to obtain the reflected and transmitted fields, the source field is represented by an angular spectrum of plane waves. With the help of Weyl's representation of the scalar Green's function [5], the electric field amplitude from Eq. (2) can be written as

$$\mathbf{E}_s(\mathbf{r}) = \frac{i\varsigma}{2\pi k_o^2} \int \mathrm{d}^2\mathbf{k}_\parallel \, \frac{1}{v_1} e^{i\mathbf{K}\cdot\mathbf{r}_1} \left[\hat{\mathbf{u}} - \frac{1}{\varepsilon_1 k_o^2} (\hat{\mathbf{u}} \cdot \mathbf{K}) \mathbf{K} \right]. \tag{5}$$

The integral runs over the $\mathbf{k}_\parallel$ plane, which is a fictitious plane that coincides with the xy plane. We adopt polar coordinates $(k_\parallel, \tilde{\phi})$ in this plane, and we set $\alpha = k_\parallel/k_o$. Convenient functions for this problem are

$$v_i = \sqrt{\varepsilon_i - \alpha^2}, \quad i = 1, 2. \tag{6}$$

We have $v_i > 0$ for $\alpha < n_i$, and for $\alpha > n_i$ this function is positive imaginary. The wave vector $\mathbf{K}$ in this representation is defined as $\mathbf{K} = \mathbf{k}_\parallel + k_o v_1 \,\mathrm{sgn}(\bar{z} + h)\mathbf{e}_z$, with $h = k_o H$ as the dimensionless distance between the dipole and the interface. For $\alpha < n_1$, e.g., $k_\parallel < n_1 k_o$, the partial wave is traveling and for $\alpha > n_1$ it is evanescent. The complex amplitude of the magnetic source field is

$$\mathbf{B}_s(\mathbf{r}) = -\frac{i\varsigma}{2\pi c k_o^3} \int \mathrm{d}^2\mathbf{k}_\parallel \, \frac{1}{v_1} e^{i\mathbf{K}\cdot\mathbf{r}_1} [\hat{\mathbf{u}} \times \mathbf{K}]. \tag{7}$$

3. Reflected and transmitted fields

The most attractive feature of the angular spectrum representation of the source field is that each partial wave (one value of $\mathbf{k}_\parallel$) is a plane-wave solution of Maxwell's equations in medium ε_1. For each such partial wave, the reflected and transmitted waves can be expressed in terms of appropriate Fresnel coefficients, and the reflected and transmitted fields then follow by superposition. For a given $\mathbf{k}_\parallel$, the fields $\mathbf{E}_s$, $\mathbf{E}_r$ and $\mathbf{E}_t$ all have the same $\mathbf{k}_\parallel$, as shown schematically in Fig. 2.

The simplest case is a dipole oscillating vertically with respect to the interface, for which $\hat{\mathbf{u}} = \mathbf{e}_z$, and in this case all partial waves of the source field are p-polarized. The system is rotationally symmetric around the z axis, and therefore we only need to consider the fields in the yz plane, with $y > 0$. The electric fields $\mathbf{E}_s$, $\mathbf{E}_r$ and $\mathbf{E}_t$ are in the yz plane, and the magnetic fields are along the x axis. The Fresnel reflection and transmission coefficients are

$$R_p(\alpha) = \frac{\varepsilon_2 v_1 - \varepsilon_1 v_2}{\varepsilon_2 v_1 + \varepsilon_1 v_2}, \tag{8}$$

$$T_p(\alpha) = \frac{n_2}{n_1} \frac{2\varepsilon_1 v_1}{\varepsilon_2 v_1 + \varepsilon_1 v_2}, \tag{9}$$

where the α dependence enters through v_1 and v_2. The reflected and transmitted fields are angular spectra, as in Eqs. (5) and (7). For the integrals over the $\mathbf{k}_\parallel$ plane we use polar coordinates $(k_\parallel, \tilde{\phi})$. The integrals over angle $\tilde{\phi}$ can be expressed in terms of Bessel functions. We introduce the associated functions r_p and t_p as

$$r_{\rm p}(\alpha,\bar{z}) = R_{\rm p} e^{iv_1(h-\bar{z})}, \tag{10}$$

$$t_{\rm p}(\alpha,\bar{z}) = T'_{\rm p} e^{i(v_1 h + v_2 \bar{z})}, \tag{11}$$

with $T'_{\rm p} = T_{\rm p}/v_1$. For the reflected fields we obtain

$$\mathbf{E}_{\rm r}(\mathbf{r}) = \frac{\varsigma}{\varepsilon_1}\int_0^\infty {\rm d}\alpha\, \alpha^2 r_{\rm p}\left[\mathbf{e}_z \frac{i\alpha}{v_1} J_0 - \mathbf{e}_y J_1\right], \tag{12}$$

$$\mathbf{B}_{\rm r}(\mathbf{r}) = -\frac{\varsigma}{c}\mathbf{e}_x \int_0^\infty {\rm d}\alpha\, \frac{\alpha^2}{v_1} r_{\rm p} J_1, \tag{13}$$

and the transmitted fields are

$$\mathbf{E}_{\rm t}(\mathbf{r}) = \frac{\varsigma}{n_1 n_2}\int_0^\infty {\rm d}\alpha\, \alpha^2 t_{\rm p}[\mathbf{e}_z i\alpha J_0 + \mathbf{e}_y v_2 J_1], \tag{14}$$

$$\mathbf{B}_{\rm t}(\mathbf{r}) = -\frac{\varsigma}{c}\mathbf{e}_x \frac{n_2}{n_1}\int_0^\infty {\rm d}\alpha\, \alpha^2 t_{\rm p} J_1. \tag{15}$$

The argument of each Bessel functions J_n is $\alpha\bar{y}$. Eqs. (12)–(15) give the reflected and transmitted fields at the field point $\mathbf{r}$, and they are functions of $\bar{y}$ and $\bar{z}$ only. The integrations over α are done numerically. We have verified that these results agree with Ref. [6], although the appearance there is quite different.

4. Field lines of the Poynting vector

The complex amplitude of the electric field in $z<0$ is $\mathbf{E} = \mathbf{E}_{\rm s} + \mathbf{E}_{\rm r}$, and similarly for the magnetic field. In $z>0$ we only have the transmitted field. The time-averaged Poynting vector is defined as

$$\mathbf{S}(\mathbf{r}) = \frac{1}{2\mu_{\rm o}}\,{\rm Re}\big[\mathbf{E}(\mathbf{r})^* \times \mathbf{B}(\mathbf{r})\big]. \tag{16}$$

This defines a vector field, and the field lines of this vector field are the flow lines of energy. With the expressions above, $\mathbf{S}(\mathbf{r})$ can be found for field points in the yz plane. Vector $\mathbf{S}(\mathbf{r})$ is in the yz plane for all $\mathbf{r}$, and therefore the field lines are 2D curves in this plane. If we parametrize a field line as $\mathbf{r}(u)$, with u a running variable, then the field lines are solutions of ${\rm d}\mathbf{r}/{\rm d}u = \mathbf{S}$. A field line through a given point $(\bar{y}_{\rm o}, \bar{z}_{\rm o})$ in the $\bar{y}\bar{z}$ plane (in dimensionless variables) can be obtained by numerical integration of ${\rm d}\mathbf{r}/{\rm d}u = \mathbf{S}$ with $(\bar{y}_{\rm o}, \bar{z}_{\rm o})$ as initial value.

For a field point on the z axis we have $\hat{\mathbf{q}}_1 = {\rm sgn}(\bar{z}+h)\mathbf{e}_z$, and since $\hat{\mathbf{u}} = \mathbf{e}_z$ we have $\hat{\mathbf{q}}_1 \times \hat{\mathbf{u}} = 0$. It then follows from Eq. (4) that $\mathbf{B}_{\rm s} = 0$. For the reflected and transmitted fields we have $J_1(0) = 0$ in Eqs. (13) and (15). Therefore, the magnetic field vanishes on the z axis, and the Poynting vector is zero. The z axis is a singular line in the flow pattern of energy.

5. Transmission into a thicker medium

When a linear dipole is embedded in an infinite medium with index of refraction n_1, the field lines of the Poynting vector are straight. Fig. 3 shows the field lines of energy flow for a dipole in a medium with $n_1 = 1$, and the material in $z>0$ has index of refraction $n_2 = 2$. The dipole is located at $h = 2$, which is a fraction of a wavelength from the interface. In the region $\bar{z}<0$, the field lines come out of the dipole, and they are slightly curved. This curving is a result of interference with the reflected field, and this is very similar to the wiggling of the field lines in $\bar{z}<0$ in Fig. 1. The field lines of the transmitted field in $\bar{z}>0$ are nearly straight and parallel, and they bend to the normal, as compared to the incident field lines. This could be expected for transmission into a thicker medium. The parallel flow lines in $\bar{z}>0$ in Fig. 3 are very similar to the flow lines of the transmitted field for a plane wave (Fig. 1). For a plane wave, all radiation hits the interface under the same angle of incidence, whereas it can be seen from Fig. 3 that for dipole radiation the angle of incidence of the Poynting vector varies along the interface. At $\bar{y} = 0$, the radiation is under normal incidence ($\theta_{\rm i} = 90°$), and this angle gets smaller with increasing $\bar{y}$. Nevertheless, the transmission angle $\theta_{\rm t}$ appears to be the same along the interface. Clearly, $\theta_{\rm t}$ is not determined by the angle of incidence (and the indices of refraction), as in Snell's law.

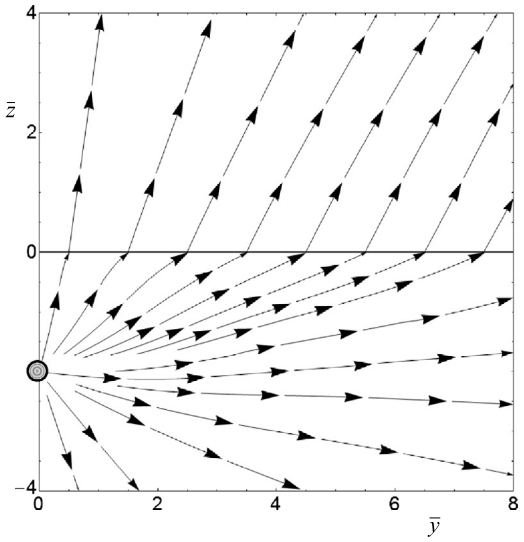

Fig. 3. The figure shows the flow lines of energy for a dipole embedded in a medium with index of refraction $n_1 = 1$, and located near an interface with a medium with index of refraction $n_2 = 2$. The transmitted flow lines leave the interface approximately under the critical angle (30° for this case), except near the z axis.

The transmitted field is a superposition of plane waves, as given by the angular spectrum representation. The weight of each partial wave is determined by the (reduced) Fresnel coefficient $T'_{\rm p}$. This Fresnel coefficient is a function of α, which is related to the angle of incidence as $\alpha = n_1 \sin\theta_{\rm i}$. Since the transmitted wave has the same α, we also have $\alpha = n_2 \sin\theta_{\rm t}$, and this yields Snell's law. For $n_2 > n_1$ we have $\theta_{\rm t} < \theta_{\rm i}$. The critical angle $\theta_{\rm c}$ for this case is the transmission angle corresponding to an angle of incidence of 90°. Therefore, $\sin\theta_{\rm c} = n_1/n_2$. At this angle of incidence we have $\alpha = n_1$, and with Eq. (6) this gives $v_1 = 0$. Since v_1 appears in the denominator in Eq. (9), we expect a sharp peak in $T'_{\rm p}$ at $\theta_{\rm t} = \theta_{\rm c}$. Fig. 4 shows $|T'_{\rm p}|^2$ as a function of $\theta_{\rm t}$ for $n_1 = 1$, $n_2 = 2$. We have $\theta_{\rm c} = 30°$, and there is indeed a sharp peak at the critical angle. As a result, the field lines of the transmitted field in Fig. 3 emanate from the interface under $\theta_{\rm t} = 30°$, except very close to the $\bar{z}$ axis.

The field line pattern in Fig. 3 shows the flow of energy in the near field. Experimentally, one measures the radiated power per unit solid angle, ${\rm d}P/{\rm d}\Omega$, in the far field. This radiation pattern can be obtained from the same angular spectra representations as above by asymptotic expansion [7]. Fig. 5 shows ${\rm d}P/{\rm d}\Omega$ for the same system as in Fig. 3. In the transmission region, $z>0$, there is a sharp peak in the power distribution at the critical angle, and there is almost no radiated power in the region $z<0$. Since the system is rotation symmetric around the z axis, this peak represents a cone around the z axis. Most radiation appears to travel over the surface of this cone to the far field. It is clear from Fig. 3 that this is due to the change of direction of the field lines of energy flow at the interface.

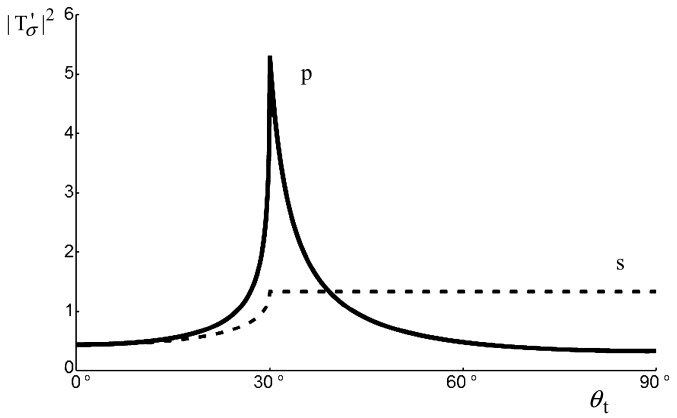

Fig. 4. Graph of $|T'_p|^2$ for a p-polarized (solid curve) plane wave as a function of the transmission angle θ_t. The indices of refraction are $n_1 = 1$ and $n_2 = 2$. The critical angle is $\theta_t = 30°$, and $|T'_p|^2$ has a sharp peak at this angle. For comparison, the dashed line is $|T'_s|^2$, the same function for s polarization.

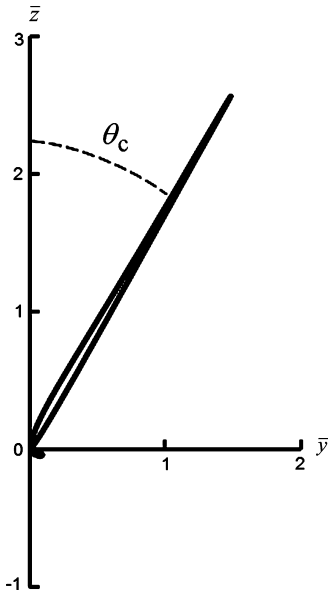

Fig. 5. The figure shows a polar diagram of the radiated power per unit solid angle for $n_1 = 1$, $n_2 = 2$ and $h = 2$.

6. Transmission into a thinner medium

Fig. 6 shows the field lines of energy flow for a dipole near an interface with a thinner medium. The dipole is located at $h = 2$, and the indices of refraction are $n_1 = 2$ and $n_2 = 1$. Close to the dipole, the field lines bend away from the normal when passing through the interface, just like optical rays. But then, in the thinner medium some field lines curve towards the interface, and cross the interface again. Once in $z < 0$, they turn around again, and this pattern repeats itself. We see that radiation near the interface oscillates back and forth through the interface. The far-field intensity distribution is shown in Fig. 7. There are two interference maxima in the reflection region, and hardly any radiation ends up in the transmitted far field.

An enlargement of the region around the first crossing of field lines with the interface is shown in Fig. 8. Field lines that enter this area from the left split at the point indicated by the white circle. Since at this point the direction of the Poynting vector is undetermined, it must be a singularity where $\mathbf{S} = 0$. Below this point, some field lines form closed loops. These loops form an optical vortex, and there has to be a singular point at the center. Since the system is rotation symmetric around the z axis, these loops are cross sections of a torus with the z axis at the center. The oscillating pattern repeats for large $\bar{y}$, and therefore there is a set of concentric vortex tori around the z axis, and just above the interface.

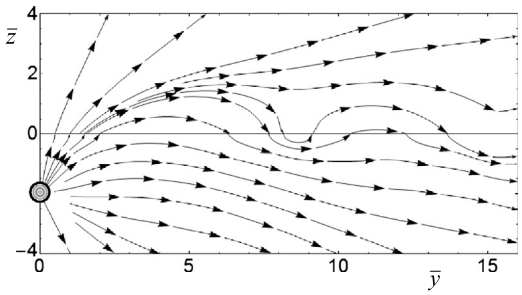

Fig. 6. The figure shows the energy flow pattern for $n_1 = 2$, $n_2 = 1$ and $h = 2$. Near the interface, the energy oscillates back and forth through the interface.

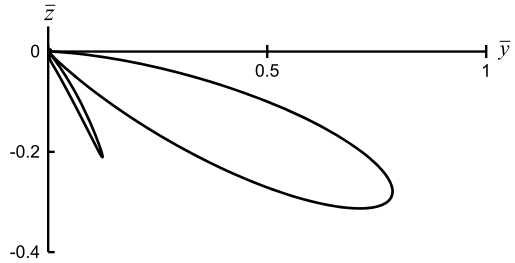

Fig. 7. Polar diagram of $\mathrm{d}P/\mathrm{d}\Omega$ for $n_1 = 2$, $n_2 = 1$ and $h = 2$.

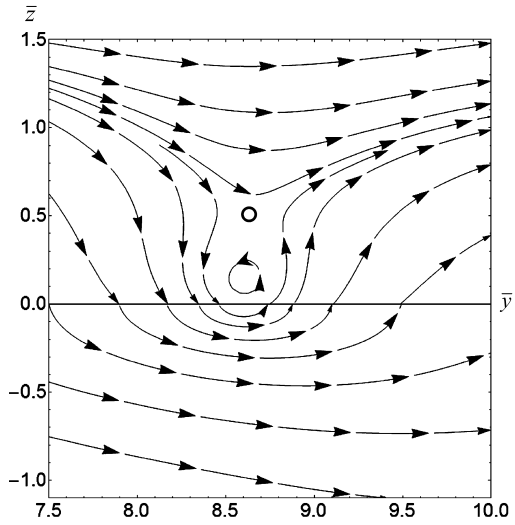

Fig. 8. The figure shows an enlargement of a part of Fig. 6. Field lines of energy flow that have crossed the interface return to the lower medium, and then curve back up to the upper medium. Above the dip below the interface, an optical vortex appears.

7. Location of the vortices

At the center of a vortex is a singularity where $\mathbf{S} = 0$. The Poynting vector vanishes when $\mathbf{E} = 0$, $\mathbf{B} = 0$ or $\mathbf{E}^* \times \mathbf{B}$ imaginary. In the yz plane, $\mathbf{E}$ is in the yz plane, $\mathbf{B}$ is along the x axis, and $\mathbf{S}$ is in the yz plane. Since $\mathbf{E}$ and $\mathbf{B}$ are complex amplitudes, they vanish when their real and imaginary parts are zero at the same point. Therefore, it is highly unlikely that $\mathbf{E} = 0$, since this would

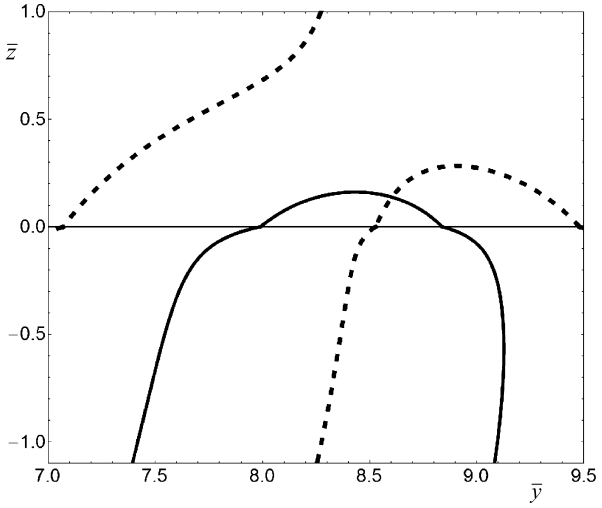

Fig. 9. The solid curve represents the solution of $\mathrm{Re}\, B_x = 0$, and on the dashed curves we have $\mathrm{Im}\, B_x = 0$. At an intersection of a solid curve and a dashed curve, the magnetic field vanishes and the Poynting vector has a singularity. This singularity is at the center of a vortex.

require four functions to vanish simultaneously. We now consider $\mathbf{B} = 0$. For this to occur we must have $\mathrm{Re}\, B_x = 0$ and $\mathrm{Re}\, B_y = 0$. Each equation defines a set of curves in the yz plane, and the magnetic field vanishes at intersections of these curves. Along the solid curve in Fig. 9 we have $\mathrm{Re}\, B_x = 0$, and along the dashed curves the imaginary part of B_x vanishes. The solid and dashed curves intersect at one point in the figure, and it is seen that this is the location of the center of the vortex in Fig. 8. For larger values of $\bar{y}$, the curves in Fig. 9 repeat, and each intersection represents the center of a vortex. Again, the system is rotation symmetric around the z axis, so these intersections represent concentric circles around the z axis.

The singularity indicated by the little circle in Fig. 8 is apparently not due to the vanishing of the magnetic field. At such singular points, where field lines split, $\mathbf{E}^* \times \mathbf{B}$ is imaginary.

8. Conclusions

We have considered the radiation emitted by a vertical electric dipole in the vicinity of an interface with a dielectric, and in particular the transmission of the radiation through the interface. When the radiation transmits into a thicker medium, it appears that the angle of transmission is determined by the Fresnel transmission coefficient, and not by the angle of incidence (as in ray optics). After passing through the interface, the radiation travels along (approximately) straight lines to the far field, and the redirection at the interface is responsible for the angular power distribution in the far field. For transmission into a thinner medium, it appears that some of the energy that passes through the interface keeps on oscillating back and forth through the interface. Just above a point where the energy flow lines dips back into the lower medium, an optical vortex appears. These vortices form a set of concentric tori around the z axis, and they are located just above the interface in the thinner medium. At the centers are singular circles, at which the magnetic field vanishes.

References

[1] F. Goos, H. Hänchen, Ann. Phys. 436 (1947) 333.
[2] H. Wolter, Z. Naturforsch. A, J. Phys. Sci. 5 (1950) 278;
translated in H. Wolter, J. Opt. A, Pure Appl. Opt. 11 (2009) 090401.
[3] X. Li, H.F. Arnoldus, Opt. Commun. 305 (2013) 76.
[4] X. Li, H.F. Arnoldus, Phys. Rev. A 81 (2010) 053844.
[5] L. Mandel, E. Wolf, Optical Coherence and Quantum Optics, Cambridge University Press, Cambridge, New York, 1995, Sec. 3.2.4.
[6] L. Novotny, B. Hecht, Principles of Nano-Optics, Cambridge University Press, Cambridge, New York, 2006.
[7] H.F. Arnoldus, J.T. Foley, J. Opt. Soc. Am. A 21 (2004) 1109.